Eur Radiol (2017) 27:354–364
DOI 10.1007/s00330-016-4323-5

MAGNETIC RESONANCE

# Non-enhanced magnetic resonance imaging of unruptured intracranial aneurysms at 7 Tesla: Comparison with digital subtraction angiography

**Karsten H. Wrede[1,2] · Toshinori Matsushige[1,2,3] · Sophia L. Goericke[4] · Bixia Chen[1,2] · Lale Umutlu[4] · Harald H. Quick[1,5] · Mark E. Ladd[1,4,6] · Sören Johst[1] · Michael Forsting[4] · Ulrich Sure[2] · Marc Schlamann[4,7]**

Received: 10 November 2015 / Revised: 2 March 2016 / Accepted: 5 March 2016 / Published online: 18 March 2016


**Abstract**

*Purpose* To prospectively evaluate non-contrast-enhanced 7-Tesla (T) MRA for delineation of unruptured intracranial aneurysms (UIAs) in comparison with DSA.

*Material and methods* Forty patients with single or multiple UIAs were enrolled in this IRB-approved trial. Sequences acquired at 7 T were TOF MRA and non-contrast-enhanced MPRAGE. All patients additionally underwent 3D rotational DSA. Two neuroradiologists individually analysed the following aneurysm and image features on a five-point scale in 2D and 3D image reconstructions: delineation of parent vessel, dome and neck; overall image quality; presence of artefacts. Interobserver accordance was assessed by the kappa coefficient.

*Results* A total of 64 UIAs were detected in DSA and in all 2D and 3D MRA image reconstructions. Ratings showed comparable results for DSA and 7-T MRA when considering all image reconstructions. Highest ratings for individual image reconstructions were given for 2D MPRAGE and 3D TOF MRA. Interobserver accordance was almost perfect for the majority of ratings.

*Conclusion* This study demonstrates excellent delineation of UIAs using 7-T MRA within a clinical setting comparable to the gold standard, DSA. The combination of 7-T non-enhanced MPRAGE and TOF MRA for assessment of untreated UIAs is a promising clinical application of ultra-high-field MRA.

*Key Points*

- *Non-enhanced 7-T MRA allowed excellent delineation of unruptured intracranial aneurysms (UIAs).*
- *Image quality at 7-T was comparable with DSA considering both sequences.*
- *Assessment of UIAs is a promising clinical application of ultra-high-field MRA.*

**Keywords** Magnetic resonance angiography · Time-of-flight · MPRAGE · 7-T · Unruptured intracranial aneurysm

✉ Karsten H. Wrede
karsten.wrede@uk-essen.de

1 Erwin L. Hahn Institute for Magnetic Resonance Imaging, University Duisburg-Essen, 45141 Essen, Germany

2 Department of Neurosurgery, University Hospital Essen, Hufelandstrasse 55, 45147 Essen, Germany

3 Department of Neurosurgery, Graduate School of Biomedical and Health Sciences, Hiroshima University, 734-8553, Hiroshima, Japan

4 Department of Diagnostic and Interventional Radiology and Neuroradiology, University Hospital Essen, 45147 Essen, Germany

5 High Field and Hybrid MR Imaging, University Hospital Essen, 45147 Essen, Germany

6 Division of Medical Physics in Radiology (E020), German Cancer Research Center (DKFZ), 69120 Heidelberg, Germany

7 Department of Neuroradiology, University Hospital Giessen, 35385 Giessen, Germany

**Abbreviations**

| | |
|---|---|
| 7-T | 7-Tesla |
| CNR | Contrast-to-noise ratio |
| DSA | Digital subtraction angiography |
| FWER | Familywise error rate |
| GRAPPA | Generalized Autocalibrating Partial Parallel Acquisition |
| MPRAGE | Magnetization-prepared rapid acquisition gradient-echo |

| | |
|---|---|
| MRA | Magnetic resonance angiography |
| PACS | Picture Archiving and Communication System |
| RF | Radiofrequency |
| SAH | Subarachnoid haemorrhage |
| SEM | Standard error of mean |
| SNR | Signal-to-noise ratio |
| TOF | Time-of-flight |
| TONE | Tilt-optimized non-saturated excitation |
| UIA | Unruptured intracranial aneurysm |

## Introduction

Subarachnoid haemorrhages (SAHs) are responsible for 25 % of all cerebrovascular-related deaths [1] and are related to intracranial aneurysm rupture in approximately 80 % of all cases. More than 30 % of surviving patients suffer from high morbidity due to intra-parenchymatous bleedings accompanying initial aneurysm rupture or consecutive vasospasms leading to cerebral infarctions. Only one-third of all patients with aneurysmal SAH are ultimately able to fully return to work, and one-third work fewer hours or in less responsible positions [2, 3]. Previous studies have shown that size and shape of unruptured intracranial aneurysms (UIAs) significantly influences the rupture rate. Therefore, high-quality delineation of UIAs plays an important role for indication, planning and execution of UIA treatment [4–6].

The current gold standard for detection of UIA remains digital subtraction angiography (DSA). Nevertheless, ionizing radiation, iodinated contrast agent as well as the general risk of an invasive diagnostic procedure have to be taken into consideration, as DSA is associated with a risk for severe permanent neurological complications. Publications including data from the last three decades [7, 8] report risks as high as 0.2–0.5 %. However, today's complication rates might be lower due to technical advances and softer catheters. Within the past two decades, magnetic resonance angiography (MRA) has become an excellent non-invasive diagnostic alternative to DSA. Sensitivity rates between 79 % and 97 % have been reported for 1.5-T (T) MRA for detection of small UIAs [9–12]. Even better performance has been shown for 3- and 7-T (ultra-) highfield non-enhanced MRA, with recent studies reporting sensitivity rates comparable with the gold standard DSA [13–16]. Increased signal-to-noise (SNR) and contrast-to-noise (CNR) ratios at higher magnetic field strength lead to improved spatial resolution and vessel contrast. One major limitation of 7-T TOF MRA is posed by SAR restrictions. Thus, optimized pulse sequences were developed allowing reasonable acquisition times while providing excellent image contrast [17, 18]. Several studies comparing 7-T MRA to lower field strength MRA have recently been published and have shown feasibility and superior image quality for 7-T MRA [19–23]. For treatment decisions, not only the detection and the size of UIAs is important. The microarchitecture of an UIA such as daughter lesions or adjacent small vessels, assessable by 1.5- and 3-T MRI only with strong limitations, is also extremely relevant.

The purpose of this prospective study was to evaluate diagnostic application and image quality for assessment of UIA by ultra-high-field 7-T TOF MRA and non-enhanced MPRAGE imaging in comparison to the current gold standard DSA within a clinical setting.

## Materials and methods

### Ethics statement

The study was conducted according to the principles of the Declaration of Helsinki and was approved by the local university institutional review board. Written informed consent was obtained before each examination.

### Study design and population

The study group comprised 40 neurosurgical patients, displaying a total of 64 UIAs (male n = 15, female n = 25; average age 58 years, standard error of mean (SEM) 1.6; range 38–80 years). Inclusion criteria were: (1) single or multiple UIAs, (2) age >18 years, (3) ability to provide informed consent and (4) legal competence. Exclusion criteria were: (1) need for monitoring on intensive care or intermediate care unit as well MR-related contraindications including (2) cardiac pacemakers or any other electronic implants, (3) all metallic implants including titanium aneurysm clips and Guglielmi detachable coils, (4) pregnancy, (5) claustrophobia and (6) chronic or episodic vertigo.

### MRI scanner and coil system

Ultra-high-field examinations were acquired on a 7-T whole-body MRI system (Magnetom 7 T, Siemens Healthcare GmbH, Erlangen, Germany) with a 32-channel Tx/Rx radiofrequency (RF) head coil (Nova Medical, Wilmington, MA, USA). The gradient system of the scanner provides a maximum amplitude of 45 mT/m and a slew rate of 200 mT/m/ms. Prior to acquisition of diagnostic sequences $B_0$-shimming was performed using a vendor-provided gradient echo sequence and algorithm. For $B_1$-field mapping and local flip angle optimization a vendor-provided spin-echo type sequence was used; after a slice selective excitation, two refocusing pulses generate a spin-echo and a stimulated echo.

### Time-of-flight (TOF) MRA sequence

The TOF MRA sequence was based on a 3D FLASH sequence with flow compensation and tilt-optimized non-saturated excitation (TONE) across the slab [17, 24]. Datasets were acquired with an excitation flip angle of $\alpha = 18°$, TE = 4.34 ms, TR = 20 ms, FOV $200 \times 169 \times 46$ mm$^3$, 112 slices per slab (oversampling 14 %), Generalized Autocalibrating Partial Parallel Acquisition (GRAPPA) acceleration factor R = 4 (phase direction), partial Fourier 6/8 in both slice and phase directions, matrix of $896 \times 756$ (non-interpolated), and a voxel size of $0.22 \times 0.22 \times 0.41$ mm$^3$ in a total acquisition time of 6 min 22 s. To ameliorate SAR restrictions, the variable-rate selective excitation algorithm [17] was used for both excitation and saturation RF pulses. Additionally, the flip angle of the saturation RF pulses was reduced from 90° to 35° – which leads to sufficient venous saturation for the given TR [18, 19]. The vendor-provided system was used for SAR monitoring.

### Magnetization-prepared rapid acquisition gradient-echo (MPRAGE) sequence

The following parameters were applied for MPRAGE imaging: TR = 2500 ms, TE = 1.54 ms, TI = 1100 ms, TA = 6 min 13 s, GRAPPA acceleration factor R = 2, excitation flip angle $\alpha = 7°$, adiabatic wideband, uniform rate, smooth truncation pulse for magnetization preparation [25], bandwidth = 570 Hz/px, 256 slices per slab (slice oversampling 75 %), matrix $384 \times 336$ (non-interpolated), FOV = $270 \times 236$ mm$^2$, voxel size $0.7 \times 0.7 \times 0.7$ mm$^3$ leading to a total acquisition time of 6 min 13 s.

### Digital subtraction angiography

Four-vessel DSA was performed using a Philips Allura angiography suite (Philips Healthcare, Best, The Netherlands) capable of 3-dimensional (3D) rotational DSA. After the standardized introduction, the previously performed 'oblique' two-plane projections of the posterior circulatory system and both internal carotid artery circulation areas were typically replaced by the relevant rotational series resulting in a reduction of radiation exposure for patients and examiners. The 3D DSA scans were acquired over a period of 4.1 s with a C-arm rotation of 240°. The injection of 18 ml of iodinated contrast agent with a flow rate of 3 ml/s into the ACI and 15 ml of contrast agent with a flow rate of 2 ml/s in the posterior circulatory system was performed automatically with the help of an injector (MedRad, Mark V ProVis®, MEDRAD Medizinische Systeme GmbH, Volkach, Germany). During the rotation, 122 images were acquired and used to create 3D image reconstructions that were send to the Picture Archiving and Communication System (PACS) along with the 'fluoroscopy images' for evaluation by both raters. After evaluation of the 3D images a targeted projection of the aneurysm was performed in a conventional DSA series.

### Three-dimensional MR image reconstruction

Prior to 2-dimensional (2D) and 3D image reconstruction N4 heterogeneity correction [26] was applied to TOF and MPRAGE datasets to correct for considerable intensity bias fields due to $B_1$-field heterogeneity. High-resolution 2D and 3D image reconstructions were then rendered using the MeVisLab image processing framework and visual development environment (http://www.mevislab.de/). Screenshots were taken from all rated 2D and 3D visualizations and were archived for potential later reassessment. Image reconstructions were defined as follows: 2D multiplanar image reconstruction of TOF MRA (2D TOF MRA); 2D multiplanar image reconstruction of MPRAGE (2D MPRAGE); 3D maximum intensity projection of TOF MRA (3D TOF MRA); 3D maximum intensity projection of MPRAGE (3D MPRAGE).

### Image evaluation and statistics

Image evaluation was performed separately and independently by two experienced neuroradiologists for all individual 2D and 3D image reconstructions of both MRI sequences, a combination of all four MRI image reconstructions (combined 7 T), as well as for DSA images. The total number of UIAs, location and lateralization were assessed. Both readers individually evaluated the following features for qualitative analysis utilizing a five-point scale (5 = excellent, 4 = good, 3 = moderate, 2 = poor, and 1 = non-diagnostic vessel delineation):

1. Delineation of parent vessel
2. Delineation of aneurysm dome
3. Delineation of aneurysm neck
4. Overall image quality
5. Presence of artefacts

Interobserver accordance for ordinal scale variables was assessed using the kappa coefficient [27] (k) according to Landis [28] as follows: Poor (k < 0.00), Slight (k = 0.00-0.20), Fair (k = 0.21-0.40), Moderate (k = 0.41-0.60), Substantial (k = 0.61-0.80), Almost Perfect (k = 0.81-1.00).

For intermethod comparisons the Wilcoxon matched-pairs two-sided signed-ranks test was applied. To control familywise error rate (FWER) due to multiple testing, several procedures were sequentially used. As the first step, the overall significance level $\alpha$ was set to 0.01 after applying a Bonferroni correction to account for five rated individual aneurysm/image features. To control FWER due to multiple

**Table 1** Basic demographic data of patients with single aneurysms: aneurysm location, side, width of aneurysm neck, height of aneurysm dome and maximal diameter of aneurysm sack

| Aneurysm | Subject | Sex | Age | Location | Side | Neck* (mm) | Height* (mm) | Diameter* (mm) |
|---|---|---|---|---|---|---|---|---|
| 1 | 1 | Male | 47 | BA | | 5.3 | 5.3 | 6.7 |
| 2 | 2 | Female | 52 | ICA | Left | 6.2 | 6.4 | 8.1 |
| 3 | 3 | Female | 43 | MCA | Right | 2.6 | 4.1 | 3.7 |
| 4 | 4 | Female | 56 | ICA | Right | 10.5 | 31.1 | 37.4 |
| 5 | 5 | Female | 61 | MCA | Left | 3.2 | 4.0 | 3.9 |
| 6 | 6 | Female | 56 | MCA | Right | 7.8 | 6.5 | 8.7 |
| 7 | 7 | Male | 70 | BA | | 8.2 | 4.5 | 8.8 |
| 8 | 8 | Male | 45 | PCA | Left | 3.3 | 14.3 | 20.0 |
| 9 | 9 | Female | 54 | MCA | Right | 4.4 | 4.4 | 7.2 |
| 10 | 10 | Female | 60 | ICA | Right | 12.8 | 13.0 | 17.0 |
| 11 | 11 | Female | 60 | MCA | Left | 3.6 | 6.8 | 7.1 |
| 12 | 12 | Female | 44 | ACA | Right | 1.4 | 2.0 | 2.5 |
| 13 | 13 | Male | 57 | BA | | 4.5 | 4.0 | 5.3 |
| 14 | 14 | Male | 60 | ACA | Left | 3.0 | 11.2 | 11.6 |
| 15 | 15 | Male | 55 | MCA | Right | 6.8 | 9.9 | 10.2 |
| 16 | 16 | Male | 49 | PC | Right | 7.6 | 9.8 | 6.7 |
| 17 | 17 | Female | 40 | MCA | Left | 7.1 | 9.3 | 8.9 |
| 18 | 18 | Female | 38 | MCA | Right | 4.2 | 7.9 | 5.9 |
| 19 | 19 | Male | 54 | SCA | Left | 0.5 | 1.1 | 0.9 |
| 20# | 20 | Male | 75 | BA | | 21.2 | 19.5 | 25.2 |
| 21# | 21 | Male | 80 | MCA | Right | 4.5 | 26.9 | 39.5 |
| 22 | 22 | Female | 53 | MCA | Right | 4.2 | 5.4 | 6.6 |
| 23 | 23 | Female | 61 | MCA | Left | 4.0 | 19.8 | 17.5 |
| 24 | 24 | Female | 51 | ICA | Left | 2.4 | 1.5 | 1.9 |
| 25 | 25 | Male | 71 | BA | | 27.2 | 10.6 | 17.8 |
| 26 | 26 | Female | 73 | AcoA | | 4.5 | 12.4 | 6.1 |
| 27 | 27 | Male | 75 | MCA | Right | 4.0 | 12.7 | 6.9 |
| 28 | 28 | Female | 63 | ICA | Right | 3.4 | 8.0 | 11.0 |
| 29 | 29 | Female | 65 | MCA | Right | 6.4 | 6.7 | 9.0 |
| 30 | 30 | Male | 56 | MCA | Right | 9.1 | 31.9 | 24.7 |

*Size in mm: Aneurysm sizes were measured in consensus reading in two orthogonal planes of maximum intensity projections. Shown are 7-T TOF MRA measurements. Wilcoxon matched-pairs two-sided signed-ranks test was calculated for all 64 aneurysms analysed in this study. There were no significant differences between TOF MRA and MPRAGE and DSA. Mean diameters with standard error of mean (SEM) and range are listed below for all patients with single aneurysms

*7-T TOF MRA*

Neck: 6.5 mm (SEM 1; 0.5–27.2 mm) Height: 10.4 mm (SEM 1.5; 1.1–31.9 mm) Diameter: 11.6 mm (SEM 1.8; 0.9–39.5 mm)

*7-T MPRAGE*

Neck: 6.6 mm (SEM 1; 0.9–25.5 mm) Height: 10.6 mm (SEM 1.5; 0.6–31.7 mm) Diameter: 11.7 mm (SEM 1.7; 0.9–39.0 mm)

*DSA*

Neck: 5.7 mm (SEM 0.9; 0.6–25.9 mm) Height: 8.7 mm (SEM 1.1; 1.3–31.5 mm) Diameter: 9.1 mm (SEM 1.3; 1–37.3 mm)

# These two aneurysms were completely thrombosed and could not be visualized by DSA

*7-T* 7-Tesla, *ACA* anterior cerebral artery, *AcoA* anterior communicating artery, *BA* basilar artery, *ICA* internal carotid artery, *MCA* middle cerebral artery, *PC* pericallosal artery, *PCA* posterior cerebral artery, *PcoA* posterior communicating artery, *PICA* posterior inferior cerebellar artery, *SCA* superior cerebellar artery, *TOF* time-of-flight, *MRA* magnetic resonance angiography, *DSA* digital subtraction angiography, *MPRAGE* magnetization-prepared rapid acquisition gradient-echo

**Table 2** Basic demographic data of patients with multiple aneurysms: aneurysm location, side, width of aneurysm neck, height of aneurysm dome and maximal diameter of aneurysm sack

| Aneurysm | Subject | Sex | Age | Location | Side | Neck* (mm) | Height* (mm) | Diameter* (mm) |
|---|---|---|---|---|---|---|---|---|
| 31 | 31 | Female | 69 | ICA | Left | 5.3 | 5.3 | 6.7 |
| 32 | | | | ICA | Left | 6.2 | 6.4 | 8.1 |
| 33 | 32 | Male | 50 | MCA | Right | 2.6 | 4.1 | 3.7 |
| 34 | | | | MCA | Left | 10.5 | 31.1 | 37.4 |
| 35 | 33 | Female | 59 | MCA | Right | 3.2 | 4.0 | 3.9 |
| 36 | | | | ICA | Left | 7.8 | 6.5 | 8.7 |
| 37 | 34 | Female | 75 | AcoA | | 8.2 | 4.5 | 8.8 |
| 38 | | | | MCA | Left | 3.3 | 14.3 | 20.0 |
| 39 | 35 | Female | 51 | BA | | 4.4 | 4.4 | 7.2 |
| 40 | | | | MCA | Right | 12.8 | 13.0 | 17.0 |
| 41 | | | | MCA | Right | 3.6 | 6.8 | 7.1 |
| 42 | 36 | Female | 52 | ICA | Right | 1.4 | 2.0 | 2.5 |
| 43 | | | | MCA | Right | 4.5 | 4.0 | 5.3 |
| 44 | | | | MCA | Left | 3.0 | 11.2 | 11.6 |
| 45 | | | | ICA | Left | 6.8 | 9.9 | 10.2 |
| 46 | 37 | Female | 52 | MCA | Right | 7.6 | 9.8 | 6.7 |
| 47 | | | | AcoA | | 7.1 | 9.3 | 8.9 |
| 48 | | | | ACA | Right | 4.2 | 7.9 | 5.9 |
| 49 | | | | ACA | Left | 0.5 | 1.1 | 0.9 |
| 50 | 38 | Male | 68 | BA | | 21.2 | 19.5 | 25.2 |
| 51 | | | | MCA | Right | 4.5 | 26.9 | 39.5 |
| 52 | | | | PcoA | Right | 4.2 | 5.4 | 6.6 |
| 53 | | | | MCA | Left | 4.0 | 19.8 | 17.5 |
| 54 | 39 | Female | 66 | MCA | Right | 2.4 | 1.5 | 1.9 |
| 55 | | | | MCA | Left | 27.2 | 10.6 | 17.8 |
| 56 | | | | MCA | Left | 4.5 | 12.4 | 6.1 |
| 57 | | | | ACA | Right | 4.0 | 12.7 | 6.9 |
| 58 | | | | PICA | Right | 3.4 | 8.0 | 11.0 |
| 59 | 40 | Female | 53 | BA | | 6.4 | 6.7 | 9.0 |
| 60 | | | | MCA | Left | 9.1 | 31.9 | 24.7 |
| 61 | | | | MCA | Left | 5.3 | 5.3 | 6.7 |
| 62 | | | | MCA | Right | 6.2 | 6.4 | 8.1 |
| 63 | | | | PcoA | Right | 2.6 | 4.1 | 3.7 |
| 64 | | | | PCA | Left | 10.5 | 31.1 | 37.4 |

*Size in mm: Aneurysm sizes were measured in consensus reading in two orthogonal planes of maximum intensity projections. Shown are 7-T TOF MRA measurements. Wilcoxon matched-pairs two-sided signed-ranks test was calculated for all 64 aneurysms analyzed in this study. There were no significant differences between TOF MRA and MPRAGE and DSA. Mean diameters with standard error of mean (SEM) and range are listed below for all patients with multiple aneurysms

*7-T TOF MRA* Neck: 3.3 mm (SEM 0.2; 1.3–6.1 mm) Height: 5.8 mm (SEM 1.1; 0.6–32.2 mm) Diameter: 6.6 mm (SEM 1.2; 1.1–35.5 mm)

*7-T MPRAGE*

Neck: 3.4 mm (SEM 0.3; 1.3–7.1 mm) Height: 5.9 mm (SEM 1.1; 0.7–32.6 mm) Diameter: 6.6 mm (SEM 1.3; 0.9–36.0 mm)

*DSA*

Neck: 3.2 mm (SEM 0.2; 1–6.7 mm) Height: 5.8 mm (SEM 1.1; 0.6–31.8 mm) Diameter: 6.4 mm (SEM 1.2; 1–35.1 mm)

*7-T* 7-Tesla, *ACA* anterior cerebral artery, *AcoA* anterior communicating artery, *BA* basilar artery, *ICA* internal carotid artery, *MCA* middle cerebral artery, *PC* pericallosal artery, *PCA* posterior cerebral artery, *PcoA* posterior communicating artery, *PICA* posterior inferior cerebellar artery, *SCA* superior cerebellar artery, *TOF* time-of-flight, *MRA* magnetic resonance angiography, *DSA* digital subtraction angiography, *MPRAGE* magnetization-prepared rapid acquisition gradient-echo

tests between six rated visualization methods a closed test procedure was implemented. The Skillings Mack test, a generalized Friedman test for multiple group comparisons with ties and equal ranks, was applied to all combinations of groups including three, four or five imaging methods. Only if the Skillings Mack test showed significant differences within groups including five imaging methods were the subgroups sequentially tested. Within the subgroups with significant differences, a pairwise testing was performed using the Wilcoxon matched-pairs two-sided signed-ranks test. As this follows the

closed test principle, significance level for pairwise testing equals the overall significance level $\alpha$ (0.01).

For every mean value the SEM ($\sigma/\sqrt{n}$) was calculated as an estimate of the population mean. Statistical analysis was carried out with the STATA software package (Stata/MP 14.1 for Mac (64-bit Intel), StataCorp, College Station, TX, USA).

## Results

The study group comprised 40 neurosurgical patients (male n = 15, female n = 25; average age 58 years, SEM 1.6; range 38–80 years). All 7-T MRI examinations and DSA were performed successfully without any relevant side effects. Both readers identified 64 UIAs in all 2D and 3D image reconstructions of 7-T TOF MRA and 7-T MPRAGE imaging as well as in DSA. Ten patients (male n = 2, female n = 8) had multiple UIAs with frequencies ranging between 2 and 6 UIAs. Lateralization was slightly unequal with 23 left-sided UIAs, 30 right-sided UIAs, eight basilar artery UIAs and two anterior communicating artery UIAs. The majority (n = 52, 81 %) of UIAs were located in the anterior circulation with only 12 UIAs (19 %) were located in the posterior circulation. Detailed information about patient demographics, UIA location and sizes are presented in Tables 1 and 2.

In summary, combined 7-T and DSA ratings were excellent without significant differences between the visualization methods. Both ratings were significantly higher than for all individual MRI reconstructions (2D TOF MRA, 3D TOF MRA, 2D MPRAGE and 3D MPRAGE) for all evaluated aneurysm and image features. Ratings for 2D MPRAGE and 3D TOF MRA were significantly lower, but still good to excellent for most evaluated aneurysm and image features. Evaluation of 2D TOF MRA and 3D MPRAGE resulted in the lowest ratings with a good average, but poor or non-diagnostic ratings for few specific aneurysms. Details about mean ratings for all evaluated aneurysm and image features and differences between ratings are illustrated as boxplots in Fig. 1 and are listed in Table 3. Figures 2 and 3 are exemplarily illustrating the strength and weaknesses of all four MRA image reconstructions in comparison to DSA in two patients. For the majority of ratings (n = 27) interobserver accordance was almost perfect and the remaining ratings (n = 3) showed substantial interobserver accordance. Details are shown in Table 4.

## Discussion

Non-enhanced 7-T MRA allowed excellent delineation of UIA in the presented patient cohort showing image quality comparable with DSA considering both MRA sequences. Assessment of UIAs is therefore a promising clinical application of ultra-high-field MRA and warrants further prospective research.

Digital subtraction angiography is considered to be the gold standard for evaluation and treatment planning of UIA, offering dynamic, high spatiotemporal resolution for delineation of vessel pathologies. The low clinical complication rate of DSA (<1 %) is reasonable for treatment planning (neurosurgical clipping or endovascular coiling) [8], but repetitive follow-up examinations, e.g. for monitoring of UIA, may add up to a significant cumulative complication rate [8]. Moreover, diffusion-weighted imaging studies have shown

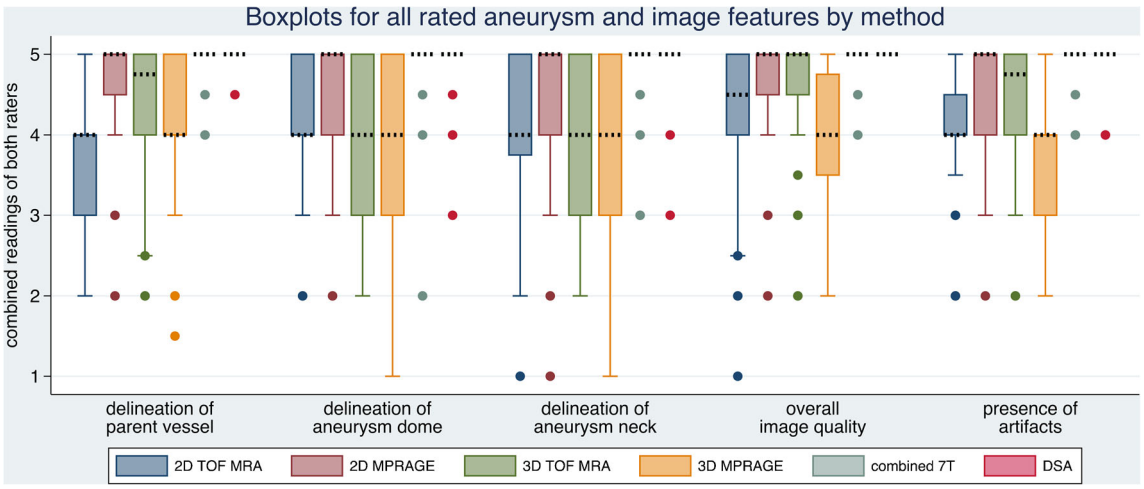


**Fig. 1** Theses box plots show combined ratings of both raters for all six imaging methods for all five rated features. Wilcoxon matched-pairs two-sided signed-ranks test showed several significant differences as well as several identities between ratings. Ratings of combined 7 Tesla and DSA showed no significant difference for all rated features and both were significantly higher ($p < 0.001$) compared to all other ratings (2D TOF MRA, 3D TOF MRA, 2D MPRAGE and 3D MPRAGE). Details of all pairwise tests are given in the results section. *DSA* digital subtraction angiography, *TOF* time-of-flight, *MPRAGE* magnetization-prepared rapid acquisition gradient-echo

**Table 3** Mean values and standard error of mean (SEM) for delineation of all five rated aneurysm and image features and result of Wilcoxon matched-pairs signed-ranks tests for equality of distributions

| Delineation of parent vessel | | | | | | |
|---|---|---|---|---|---|---|
| Mean [SEM] | 2D TOF MRA | 2D MPRAGE | 3D TOF MRA | 3D MPRAGE | Combined 7 T | DSA |
| 2D TOF MRA | 4.16 [0.12] | 0.0000 ↓ | 0.0000 ↓ | 0.1085 → | 0.0000 ↓ | 0.0000 ↓ |
| 2D MPRAGE | | 4.63 [0.09] | 0.4802 → | 0.0000 ↑ | 0.0000 ↓ | 0.0000 ↓ |
| 3D TOF MRA | | | 4.55 [0.1] | 0.0000 ↑ | 0.0000 ↓ | 0.0000 ↓ |
| 3D MPRAGE | | | | 3.96 [0.11] | 0.0000 ↓ | 0.0000 ↓ |
| Combined 7-T | | | | | 4.96 [0.02] | 0.0833 → |
| DSA | | | | | | 5.00 [0.0] |
| Delineation of aneurysm dome | | | | | | |
| Mean [SEM] | 2D TOF MRA | 2D MPRAGE | 3D TOF MRA | 3D MPRAGE | Combined 7 T | DSA |
| 2D TOF MRA | 4.09 [0.12] | 0.0023 ↑ | 0.038 [SM →] | 0.038 [SM →] | 0.0000 ↓ | 0.0000 ↓ |
| 2D MPRAGE | | 4.49 [0.1] | 0.0026 ↑ | 0.0000 ↑ | 0.0000 ↓ | 0.0002 ↓ |
| 3D TOF MRA | | | 4.02 [0.14] | 0.038 [SM →] | 0.0000 ↓ | 0.0000 ↓ |
| 3D MPRAGE | | | | 3.85 [0.14] | 0.0000 ↓ | 0.0000 ↓ |
| combined 7-T | | | | | 4.85 [0.07] | 0.4065 → |
| DSA | | | | | | 4.91 [0.04] |
| Delineation of aneurysm neck | | | | | | |
| Mean [SEM] | 2D TOF MRA | 2D MPRAGE | 3D TOF MRA | 3D MPRAGE | Combined 7 T | DSA |
| 2D TOF MRA | 3.94 [0.14] | 0.0009 ↓ | 0.278 [SM →] | 0.278 [SM →] | 0.0000 ↓ | 0.0000 ↓ |
| 2D MPRAGE | | 4.44 [0.12] | 0.0112 → | 0.0000 ↑ | 0.0000 ↓ | 0.0000 ↓ |
| 3D TOF MRA | | | 4.02 [0.13] | 0.278 [SM →] | 0.0000 ↓ | 0.0000 ↓ |
| 3D MPRAGE | | | | 3.8 [0.14] | 0.0000 ↓ | 0.0000 ↓ |
| Combined 7-T | | | | | 4.87 [0.06] | 0.3214 → |
| DSA | | | | | | 4.95 [0.04] |
| Overall image quality | | | | | | |
| Mean [SEM] | 2D TOF MRA | 2D MPRAGE | 3D TOF MRA | 3D MPRAGE | Combined 7 T | DSA |
| 2D TOF MRA | 3.96 [0.11] | 0.0000 ↓ | 0.0029 ↓ | 0.1915 → | 0.0000 ↓ | 0.0000 ↓ |
| 2D MPRAGE | | 4.6 [0.08] | 0.0117 → | 0.0000 ↑ | 0.0000 ↓ | 0.0000 ↓ |
| 3D TOF MRA | | | 4.23 [0.12] | 0.0000 ↑ | 0.0000 ↓ | 0.0000 ↓ |
| 3D MPRAGE | | | | 3.78 [0.12] | 0.0000 ↓ | 0.0000 ↓ |
| Combined 7-T | | | | | 4.95 [0.02] | 0.3214 → |
| DSA | | | | | | 4.94 [0.03] |
| Presence of artifacts | | | | | | |
| Mean [SEM] | 2D TOF MRA | 2D MPRAGE | 3D TOF MRA | 3D MPRAGE | Combined 7 T | DSA |
| 2D TOF MRA | 3.84 [0.11] | 0.0000 ↓ | 0.0029 ↓ | 0.0192 → | 0.0000 ↓ | 0.0000 ↓ |
| 2D MPRAGE | | 4.67 [0.08] | 0.0154 → | 0.0000 ↑ | 0.0009 ↓ | 0.0000 ↓ |
| 3D TOF MRA | | | 4.34 [0.11] | 0.0000 ↑ | 0.0000 ↓ | 0.0000 ↓ |
| 3D MPRAGE | | | | 4.15 [0.12] | 0.0000 ↓ | 0.0000 ↓ |
| Combined 7-T | | | | | 4.94 [0.03] | 0.0984 → |
| DSA | | | | | | 4.99 [0.01] |

Rating scale: 5 = excellent; 4 = good; 3 = moderate; 2 = poor; 1 = non-diagnostic vessel delineation

Overall significance level $\alpha$ was set to $p \leq 0.01$ after Bonferroni correction for multiple testing of five aneurysm features (delineation of parent vessel, dome and neck, overall image quality and artifacts) and closed test procedure using the Skillings Mack test

↑ Method in the first column has significant higher mean value for ratings compared to method in first line

→ No significant difference between mean values for ratings of method in the first column and method in first line

↓ Method in the first column has significant lower mean value for ratings compared to method in first line

[SM →] Post-hoc Wilcoxon matched-pairs signed-ranks tests wasnot conducted, as pre-hoc Skillings Mack test did not show significant differences for a group containing this null hypothesis

*7-T* 7-Tesla, *TOF* time-of-flight, *MRA* magnetic resonance angiography, *DSA* digital subtraction angiography, *MPRAGE* magnetization-prepared rapid acquisition gradient-echo

[29] that silent embolisms induced by invasive DSA are quite frequent (from 1.5 % up to >20 %), depending on the patient's arteriosclerosis status and experience of the examiner. Hence, imaging methods without the risk associated with invasive DSA that additionally avoid the application of contrast agent and ionizing radiation are highly desirable. Time-of-flight MR angiography at 1.5 T and 3 T has become a widely used, non-invasive tool for detection, assessment and follow-up of UIAs [30].

While 1.5-T TOF imaging is known to be limited for the assessment of small vessel pathologies [15], the increase of the magnetic field strength has been shown to enable superior vascular assessment at 3 T [31] and 7 T [15; 20] due to the increase in SNR and CNR. Ultra-high-field 7-T MRI has been

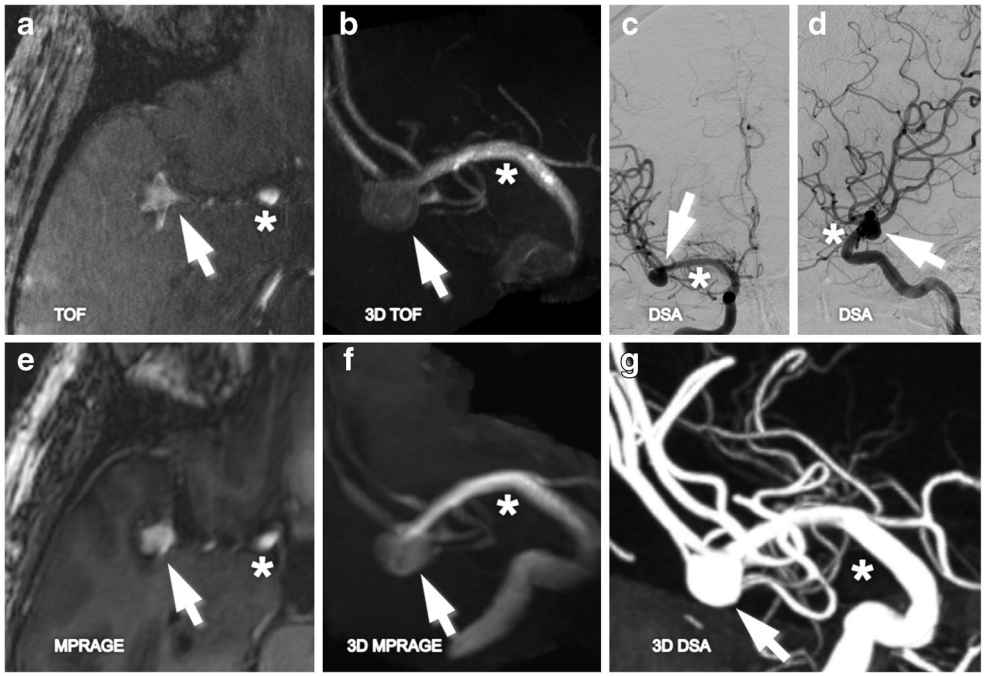


**Fig. 2** This 59-year-old female patient (subject 33) had a right MCA aneurysm and a small left ICA aneurysm. The figure shows the right-sided MCA bifurcation aneurysm (arrows) in TOF MRA (**a**), 3D maximum intensity projections of TOF MRA (**b**), DSA (anterior-posterior (**c**) and lateral (**d**) projection, MPRAGE (**e**) and 3D maximum intensity projections of MPRAGE (**f**) as well as in maximum intensity projection (**g**) of the 3D rotational DSA dataset. The asterisks are placed next to the parent vessel (M1 segment of MCA). *MCA* middle cerebral artery, *ICA* internal carotid artery, *DSA* digital subtraction angiography, *TOF* time-of-flight, *MPRAGE* magnetization-prepared rapid acquisition gradient-echo

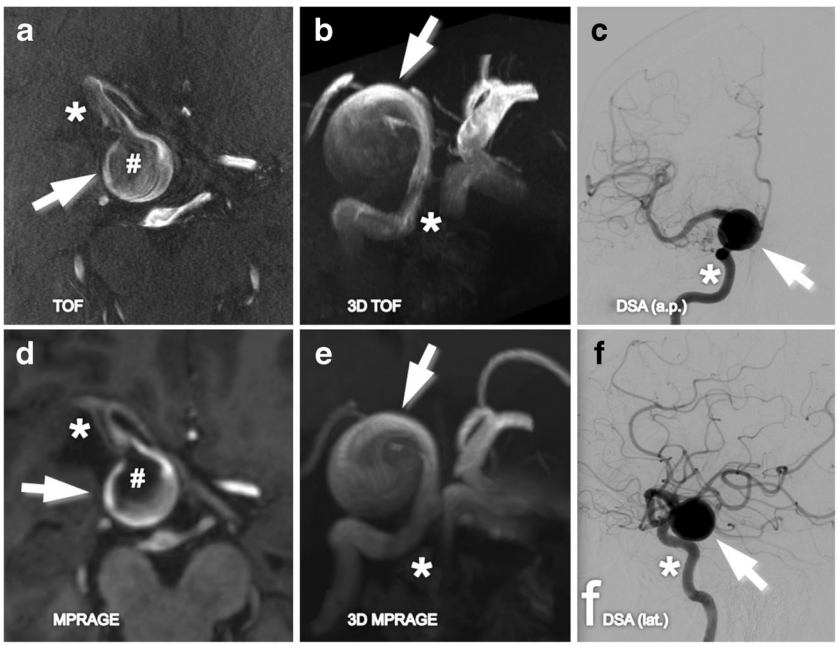


**Fig. 3** This 60-year-old female patient (subject 10) had a large right ICA aneurysm (arrows). The figure shows TOF MRA (**a**), 3D maximum intensity projections of TOF MRA (**b**), anterior-posterior (**c**) and lateral (**d**) projections of DSA as well as MPRAGE (**d**) and 3D maximum intensity projections of MPRAGE (**e**). The asterisks are placed next to the parent vessel. The number signs indicate a hypointense area within the aneurysm dome most likely caused by turbulent flow (**a**, **d**). Consideration of all four MRA image reconstructions helps to understand the vascular and aneurysm anatomy, which is difficult to fully comprehend when only evaluating a single image reconstruction. *ICA* internal carotid artery, *TOF* time-of-flight, *MRA* magnetic resonance angiography, *DSA* digital subtraction angiography, *MPRAGE* magnetization-prepared rapid acquisition gradient-echo

demonstrated to offer three beneficial features: (1) higher SNR (up to four- to fivefold higher than at 1.5 T and up to two- to threefold higher than 3 T) as well as (2) longer T1 relaxation times [32], yielding improved vessel-tissue contrast [33] and (3) inherently hyperintense arterial vasculature [34–36]. The third is most likely augmented by the application of local RF transmit coils at 7 T. Body RF coils are commonly applied for signal transmission at lower field strength. Hence, due to the local transmit coil setup at 7 T, a non-selective inversion recovery pulse is effectively a slab-selective inversion recovery pulse [36, 37]. In a recent publication, Zwawanenburg et al. [38] demonstrated the high diagnostic potential of non-enhanced MPRAGE MRI at 7 T for excellent assessment of cerebral perforating arteries and related anatomical parenchymatous structures. In two other recent studies on UIAs and intracranial arteriovenous malformations, the diagnostic potential of MPRAGE has been shown [20, 21]. Only minor non-significant improvement of vessel delineation after contrast agent application was found in a study with healthy volunteers, underlining the high diagnostic potential of non-enhanced 7-T MPRAGE MRI [34].

To prospectively evaluate diagnostic application and image quality of 7-T TOF MRA and non-enhanced MPRAGE for assessment of UIA, the presented study compares these imaging methods with the current gold standard (DSA) for the first time in a larger patient cohort.

There are some limitations of the current study that should be mentioned. The study design was intentionally focused solely on the direct comparison of 7-T MRA and the current gold standard DSA for assessment of UIAs as this comparison has not been made to date. A comparison to lower field strength MRA is of interest, but adding yet another imaging modality leads to unfavourable complexity of the statistics and reduces statistical power of the analysis. A several fold larger patient cohort would be required for a 1.5-T, 3-T, 7-T and DSA comparison study. The patient cohort was of moderate size, but very inhomogeneous and comprised of several patients with multiple UIAs. The number of aneurysms in patients with multiple UIAs accounted for half of all assessed aneurysms in this study. Thorough correction for multiple testing has been performed for the different imaging methods and the assessed image and aneurysm features, but correction for multiple UIAs in a single patient was not performed. Nevertheless, pairwise comparisons returned reasonable and consistent results. The cohort heterogeneity also had a positive effect, as UIAs in almost all locations could be assessed.

Another limitation is that especially ratings for 3D visualizations and for the combined 7-T rating are likely to depend on each observer's experience in evaluating 3D vessel reconstructions. Thus, kappa values for interobserver accordance were lower for these three imaging methods compared to 2D visualizations and DSA, but they were still substantial to almost perfect. An important limitation of all current ultra-high-field MRI studies is due to exclusion of scans in patients with most metallic implants. Despite high clinical interest for follow-up, patients after endovascular coiling or surgical clipping cannot be enrolled in 7-T MRI studies at present, as previous aneurysm treatment is still a contraindication for MRI scans >3 T. The first promising investigations on implant safety at 7 T have already been performed [39], but before patients with for example multiple UIAs (e.g. one clipped, one coiled, two conservatively observed due to very small size) can be followed up, further studies on implant safety are mandatory.

Following highly promising results when comparing 7-T MRA in UIAs to lower magnetic field strength MRA [15, 21], this study now provides the missing comparison with the current gold standard (DSA). The results of the present study show excellent assessment of UIAs for the combined rating

**Table 4** Interobserver accordance (kappa statistic) was almost perfect for the majority of ratings

| | Delineation of parent vessel | Delineation of aneurysm dome | Delineation of aneurysm neck | Overall image quality | Presence of artifacts |
|---|---|---|---|---|---|
| 2D TOF MRA | 0.88** | 0.88** | 0.98** | 0.93** | 0.98** |
| 3D TOF MRA | 0.88** | 0.95** | 0.94** | 0.95** | 0.93** |
| 2D MPRAGE | 0.96** | 0.81** | 0.88** | 0.98** | 0.98** |
| 3D MPRAGE | 0.81** | 0.97** | 0.97** | 0.97** | 0.94** |
| Combined 7-T | 0.79* | 0.95** | 0.89** | 0.65* | 0.73* |
| DSA | 1.00** | 1.00** | 1.00** | 1.00** | 1.00** |

According to Landis the kappa coefficient (k) was rated as follows:

Poor ($k < 0.00$), Slight ($k = 0.00$-$0.20$), Fair ($k = 0.21$-$0.40$), Moderate ($k = 0.41$-$0.60$)

Substantial* ($k = 0.61$-$0.80$), Almost perfect** ($k = 0.81$-$1.00$)

Disagreements were weighted by $1 - \{(i - j) / (k - 1)\}2$, where i and j index the rows and columns of the ratings by the two raters and k is the maximum number of possible ratings

*7-T* 7-Tesla, *TOF* time-of-flight, *MRA* magnetic resonance angiography, *DSA* digital subtraction angiography, *MPRAGE* magnetization-prepared rapid acquisition gradient-echo

of 2D and 3D visualizations, comparable with DSA ratings. The individual 2D and 3D ratings for TOF MRA and MPRAGE varied considerably between different image and aneurysm features. Ratings for 2D MPRAGE and 3D TOF MRA were good to excellent for most evaluated aneurysm and image features. Evaluation of 2D TOF MRA and 3D MPRAGE resulted in the lowest ratings, with a good average but low ratings for a few specific aneurysms. The variability of the ratings can be explained by specific differences between 2D and 3D reconstructions of the raw image data. The high spatial resolution of TOF MRA leads to good 3D visualizations, whereas 2D multi-planar reconstructions are prone to TOF-specific artefacts (e.g. pulsation artefacts), resulting in blurred delineation and lower ratings. The opposite is true for 2D and 3D visualizations of MPRAGE. Minimal artefacts and good vessel-tissue contrast allow excellent aneurysm depiction in 2D multi-planar image reconstructions, but significantly lower spatial resolution impairs 3D visualization. The combination of 2D and 3D TOF MRA and MPRAGE visualizations can combine the strengths of both MR sequences and overcome the weaknesses of solely 2D image reconstructions in individual cases. Consequently, ratings for aneurysm and image features are comparable with DSA ratings.

In conclusion, this study demonstrates excellent delineation of UIAs using 7-T MRA within a clinical setting. Visualization comparable to the gold standard DSA was shown for all evaluated imaging and aneurysm features for combined assessment of 2D and 3D visualizations of TOF MRA and MPRAGE. The combination of 7-T non-enhanced MPRAGE and TOF MRA for assessment of untreated UIAs is a promising clinical application of ultra-high-field MRA.

**Acknowledgements** The scientific guarantor of this publication is Dr. Karsten H. Wrede. The authors of this manuscript declare no relationships with any companies whose products or services may be related to the subject matter of the article. This study has received funding by University Duisburg Essen (IFORES grant). Dr. Ulrike Krahn kindly provided statistical advice for this manuscript. Institutional Review Board approval was obtained. Written informed consent was obtained from all subjects (patients) in this study. Methodology: prospective, observational, multicentre study.

## References

1. Fogelholm R, Hernesniemi J, Vapalahti M (1993) Impact of early surgery on outcome after aneurysmal subarachnoid hemorrhage. A population-based study. Stroke 24:1649–1654
2. Passier PE, Visser-Meily JM, Rinkel GJ, Lindeman E, Post MW (2011) Life satisfaction and return to work after aneurysmal subarachnoid hemorrhage. J Stroke Cerebrovasc Dis 20:324–329
3. Rinkel GJE, Algra A (2011) Long-term outcomes of patients with aneurysmal subarachnoid haemorrhage. Lancet Neurol 10:349–356
4. Kashiwazaki D, Kuroda S, on behalf of the Sapporo SAHSG (2013) Size ratio Can highly predict rupture risk in intracranial small (<5 mm) aneurysms. Stroke. doi:10.1161/STROKEAHA.113.001138
5. Lawson MF, Neal DW, Mocco J, Hoh BL (2013) Rationale for treating unruptured intracranial aneurysms: actuarial analysis of natural history risk versus treatment risk for coiling or clipping based on 14,050 patients in the nationwide inpatient sample database. World Neurosurg 79:472–478
6. Steinberg GK (2013) Controversy: clipping of asymptomatic intracranial aneurysm that is <7 mm: Yes. Stroke 44:S97–S99
7. Kaufmann TJ, Huston J 3rd, Mandrekar JN, Schleck CD, Thielen KR, Kallmes DF (2007) Complications of diagnostic cerebral angiography: evaluation of 19,826 consecutive patients. Radiology 243:812–819
8. Willinsky RA, Taylor SM, TerBrugge K, Farb RI, Tomlinson G, Montanera W (2003) Neurologic complications of cerebral angiography: prospective analysis of 2,899 procedures and review of the literature. Radiology 227:522–528
9. Chung TS, Joo JY, Lee SK, Chien D, Laub G (1999) Evaluation of cerebral aneurysms with high-resolution MR angiography using a section-interpolation technique: correlation with digital subtraction angiography. AJNR Am J Neuroradiol 20:229–235
10. Okahara M (2002) Diagnostic accuracy of magnetic resonance angiography for cerebral aneurysms in correlation with 3D-digital subtraction angiographic images: a study of 133 aneurysms. Stroke 33:1803–1808
11. White PM, Teasdale EM, Wardlaw JM, Easton V (2001) Intracranial aneurysms: CT angiography and MR angiography for detection prospective blinded comparison in a large patient cohort. Radiology 219:739–749
12. White PM, Teadsale E, Wardlaw JM, Easton V (2001) What is the most sensitive non-invasive imaging strategy for the diagnosis of intracranial aneurysms? J Neurol Neurosurg Psychiatry 71:322–328
13. Shahzad R, Younas F (2011) Detection and characterization of intracranial aneurysms: Magnetic resonance angiography versus digital subtraction angiography. J Coll Physicians Surg Pak 21:325–329
14. Nakiri GS, Santos AC, Abud TG, Aragon DC, Colli BO, Abud DG (2011) A comparison between magnetic resonance angiography at 3 teslas (time-of-flight and contrastenhanced) and flat-panel digital subtraction angiography in the assessment of embolized brain aneurysms. Clinics 66:641–648
15. Monninghoff C, Maderwald S, Theysohn JM et al (2009) Evaluation of intracranial aneurysms with 7 T versus 1.5 T time-of-flight MR angiography - initial experience. RoFo: Fortschr Geb Rontgenstr Nuklearmed 181:16–23
16. Ferré JC, Carsin-Nicol B, Morandi X et al (2009) Time-of-flight MR angiography at 3 T versus digital subtraction angiography in the imaging follow-up of 51 intracranial aneurysms treated with coils. Eur J Radiol 72:365–369
17. Johst S, Wrede KH, Ladd ME, Maderwald S (2012) Time-of-flight magnetic resonance angiography at 7 T using venous saturation pulses with reduced flip angles. Invest Radiol 47:445–450
18. Schmitter S, Bock M, Johst S, Auerbach EJ, Ugurbil K, Van de Moortele PF (2012) Contrast enhancement in TOF cerebral angiography at 7 T using saturation and MT pulses under SAR constraints: impact of VERSE and sparse pulses. Magn Reson Med 68:188–197
19. Matsushige T, Chen B, Dammann P et al (2015) Microanatomy of the subcallosal artery: an in-vivo 7 T magnetic resonance angiography study. Eur Radiol. doi:10.1007/s00330-015-4117-1
20. Wrede KH, Dammann P, Johst S et al (2015) Non-enhanced MR imaging of cerebral arteriovenous malformations at 7 Tesla. Eur Radiol. doi:10.1007/s00330-015-3875-0

21. Wrede KH, Dammann P, Mönninghoff C et al (2014) Non-enhanced MR imaging of cerebral aneurysms: 7 Tesla versus 1.5 Tesla. PLoS One 9:e84562
22. Martin-Vaquero P, da Costa RC, Echandi RL, Tosti CL, Knopp MV, Sammet S (2011) Time-of-flight magnetic resonance angiography of the canine brain at 3.0 Tesla and 7.0 Tesla. Am J Vet Res 72:350–356
23. Heverhagen JT, Bourekas E, Sammet S, Knopp MV, Schmalbrock P (2008) Time-of-flight magnetic resonance angiography at 7 Tesla. Invest Radiol 43:568–573
24. Wrede KH, Johst S, Dammann P et al (2014) Improved cerebral time-of-flight magnetic resonance angiography at 7 Tesla – feasibility study and preliminary results using optimized venous saturation pulses. PLoS One 9, e106697
25. Wrede KH, Johst S, Dammann P et al (2012) Caudal image contrast inversion in MPRAGE at 7 Tesla problem and solution. Acad Radiol 19:172–178
26. Tustison NJ, Avants BB, Cook PA et al (2010) N4ITK: improved N3 bias correction. IEEE Trans Med Imaging 29:1310–1320
27. Cohen J (1960) A coefficient of agreement for nominal scales. Educ Psychol Meas 20:37–46
28. Landis JR, Koch GG (1977) The measurement of observer agreement for categorical data. Biometrics 33:159–174
29. Bendszus M, Koltzenburg M, Burger R, Warmuth-Metz M, Hofmann E, Solymosi L (1999) Silent embolism in diagnostic cerebral angiography and neurointerventional procedures: a prospective study. Lancet 354:1594–1597
30. Fiehler J (2012) Unruptured brain aneurysms: when to screen and when to treat? Rofo 184:97–104
31. Gibbs GF, Huston J 3rd, Bernstein MA, Riederer SJ, Brown RD Jr (2004) Improved image quality of intracranial aneurysms: 3.0-T versus 1.5-T time-of-flight MR angiography. Am J Neuroradiol 25:84–87
32. Edelstein WA, Glover GH, Hardy CJ, Redington RW (1986) The intrinsic signal-to-noise ratio in NMR imaging. Magn Reson Med 3:604–618
33. Majoie CBLM, Sprengers ME, Van Rooij WJJ et al (2005) MR angiography at 3T versus digital subtraction angiography in the follow-up of intracranial aneurysms treated with detachable coils. Am J Neuroradiol 26:1349–1356
34. Umutlu L, Theysohn N, Maderwald S et al (2013) 7 Tesla MPRAGE imaging of the intracranial arterial vasculature: nonenhanced versus contrast-enhanced. Acad Radiol 20:628–634
35. Dammann P, Breyer T, Wrede KH et al (2014) Treatment of complex neurovascular lesions: an interdisciplinary angio suite approach. Ther Adv Neurol Disord 7:60–70
36. Grinstead JW, Rooney W, Laub G (2010) The origins of bright blood MPRAGE at 7 Tesla and a simultaneous method for T1 imaging and Non-contrast MRA. Proc Intl Soc Mag Reson Med 18:1429
37. Dammann P, Wrede KH, Maderwald S et al (2012) The venous angioarchitecture of sporadic cerebral cavernous malformations: a susceptibility weighted imaging study at 7 T MRI. J Neurol Neurosurg Psychiatry. doi:10.1136/jnnp-2012-302599
38. Zwanenburg JJ, Hendrikse J, Takahara T, Visser F, Luijten PR (2008) MR angiography of the cerebral perforating arteries with magnetization prepared anatomical reference at 7 T: comparison with time-of-flight. J Magn Reson Imaging 28:1519–1526
39. Kraff O, Wrede KH, Schoemberg T et al (2013) MR safety assessment of potential RF heating from cranial fixation plates at 7 T. Med Phys 40:042302